

2



AD-A268 733



**DEPARTMENT OF DEFENCE
DEFENCE SCIENCE AND TECHNOLOGY ORGANISATION
AERONAUTICAL RESEARCH LABORATORY**

MELBOURNE, VICTORIA

Research Report 4

**DAMAGE MONITORING IN METALLIC AND COMPOSITE
STRUCTURES USING PIEZOELECTRIC THIN FILM SENSORS**

*Some text contains color
plates: All DTIC reproduce
will be in black and
white.*

by

W.K. CHIU
S.C. GALEA

**DTIC
ELECTE
AUG 30 1993
S B D**

DISTRIBUTION STATEMENT A
Approved for public release
Distribution Unlimited

93-20043

Approved for public release.

© COMMONWEALTH OF AUSTRALIA 1993

MAY 1993

93 8 26 07 11

This work is copyright. Apart from any fair dealing for the purpose of study, research, criticism or review, as permitted under the Copyright Act, no part may be reproduced by any process without written permission. Copyright is the responsibility of the Director Publishing and Marketing, AGPS. Enquiries should be directed to the Manager, AGPS Press, Australian Government Publishing Service, GPO Box 84, CANBERRA ACT 2601.

**DEPARTMENT OF DEFENCE
DEFENCE SCIENCE AND TECHNOLOGY ORGANISATION
AERONAUTICAL RESEARCH LABORATORY**

Research Report 4

**DAMAGE MONITORING IN METALLIC AND COMPOSITE
STRUCTURES USING PIEZOELECTRIC THIN FILM SENSORS**

by

W.K. CHIU
S.C. GALEA

SUMMARY

The increasing emphasis on intelligent material systems and structures has resulted in a significant research effort in the areas of embedded and bonded sensors and actuators. Piezoelectric film are one of the many sensing materials available. The piezoelectric sensor output is proportional to changes in surface displacement and can be used to interpret variations in structural and material properties, e.g., the compliance of the structure. The aim of this paper is to demonstrate the use of piezoelectric film sensors as a structural integrity monitoring device for detecting damage in fibre reinforced composites, and crack growth in aluminium alloy specimens.



© COMMONWEALTH OF AUSTRALIA 1993

POSTAL ADDRESS: Director, Aeronautical Research Laboratory,
506 Lorimer Street, Fishermens Bend, 3207
Victoria, Australia.

TABLE OF CONTENTS

Page Nos.

1. INTRODUCTION..... 1

2. PIEZOELECTRIC THIN FILM SENSORS..... 2

3. DAMAGE IN COMPOSITE SPECIMENS 2

3.1 Experimental Setup 2

3.1.1 Impact Damaged Laminates 2

3.1.2 Composite-to-Metal Fastened Joints 3

3.2 Results and Discussion 4

3.2.1 Impact Damaged Laminates 4

3.2.2 Composite-to-Metal Fastened Joints 5

4. CRACKED METALLIC SPECIMEN..... 6

4.1 Experimental Setup 6

4.2 Numerical Analysis 6

4.3 Results and Discussions 7

5. CONCLUSIONS..... 8

ACKNOWLEDGEMENTS 8

REFERENCES..... 9

FIGURES 1-13

DISTRIBUTION

DOCUMENT CONTROL DATA

DTIC QUALITY INSPECTED 3

Accession For	
DTIS GRA&I	<input checked="" type="checkbox"/>
DTIC TAB	<input type="checkbox"/>
Unannounced	<input type="checkbox"/>
Justification	
By _____	
Distribution/ _____	
Availability Codes	
Dist	Avail and/or Special
A-1	

1. INTRODUCTION

The concept of intelligent/smart structures/materials has been the focal point of numerous recent investigations [1,2,3]. Such system contain their own sensors, actuators and control/processor capabilities and react to external stimuli in a predictable and intelligent manner. Embedded (or intrinsic) sensors recognise and measure the intensity of external or internal stimuli to which actuators can then respond. Stimuli to which these sensors respond may be either mechanical or thermal in origin. Information from the sensors can be acquired by in-situ control/processor units which then control the response of the actuators to the stimuli as well as selecting the optimum response, if a number of options are possible [1,2]. The intelligent controller also has the ability to learn from experience, and so further optimize the response.

With the increasing emphasis on intelligent materials and structures, there is significant research occurring in the areas of embedded and bonded sensors and actuators. There are currently a range of sensors and actuators available for use in smart materials and systems. The main advantages of piezoelectric materials are that they may be used as both a sensor and an actuator, and they are distributed devices. These devices generate a charge in response to mechanical stimulus or alternatively provide a mechanical strain when an electric field is applied across them. Piezoelectric materials can be crystals, ceramics or polymers, such as polyvinylidene fluoride (PVDF or PVF₂). The latter takes the form of thin sheets that can be attached to most surfaces. These materials exhibit excellent mechanical strength, low acoustic impedance and possess a flat response over a wide frequency range. Due to their low mechanical impedance a number of piezoelectric films can be distributed along a structure without drastically affecting its mechanical properties. These films can be readily cut and shaped to conform to the structure under consideration.

This paper addresses the use of piezoelectric film as a sensing device to detect:

1. damage growth in fibre reinforced plastic specimens,
2. crack growth in a centre notched aluminium specimen.

The damage growth in the composite test specimen was monitored using ultrasonic C-scanning and compared with the piezoelectric sensor readings. The crack growth due to the constant amplitude cyclic loading of the aluminium specimen was monitored with a travelling microscope and piezoelectric sensors bonded to the surface of the specimen. The variation in piezoelectric sensor output, resulting from the change in crack length, was also modelled using a finite element analysis.

2. PIEZOELECTRIC THIN FILM SENSORS

The piezoelectric sensors used in the experiments reported in this paper were made from polyvinylidene fluoride (PVDF) films. The electromechanical properties of these films are anisotropic [4]. Therefore, the electrical responses of the film differ depending on the direction of the applied mechanical load. The open circuit polarity of a piezoelectric sensor can be expressed as [5];

$$V = K_1\sigma_{1f} + K_2\sigma_{2f} \quad (1)$$

where V is the sensor output, K_1 and K_2 are the piezoelectric constants and σ_{1f} and σ_{2f} are the stresses in the piezoelectric film. Here the subscripts 1 and 2 denote the sensor's maximum sensitivity direction and that perpendicular to the sensor's maximum sensitivity direction, respectively. The constant K_1 is approximately 8 times that of K_2 . The significance of equation (1) will be discussed in section 4 where the output of a particular sensor is predicted and compared to that obtained experimentally.

3. DAMAGE IN COMPOSITE SPECIMENS

The material studied in the present work was the carbon fibre/epoxy resin system, AS4/3501-6, as a 6.7mm thick 50 ply laminate of layup $[(\pm 45_2, 0_4)_3, 90]_s$.

3.1 Experimental Setup

3.1.1 Impact Damaged Laminates

Damage growth experiments were undertaken using 300 x 100 x 6.7 mm composite coupons. A centrally located region of impact damage was introduced to represent barely visible impact damage (BVID). The absorbed impact energy was 8 J with the area of damage restrained to a diameter of 30 mm.

A number of piezoelectric sensors were made from sheets of 28 μm thick polyvinylidene fluoride film. The PVDF film, as supplied, was coated on both sides with a thin layer of vacuum deposited conductive NiCu or NiCr metal [4]. Thin electrical wires were bonded to the top and bottom surfaces by using conductive silver-loaded epoxy. The piezoelectric sensors were applied to the non-impact side of the coupon using Perma Bond F toughened acrylic adhesive. Coupon 02-05 has two, 28 μm thick, PVDF NiCr sensors located as shown in Figure 1, with sensors PZF1 and PZF2 having their directions of maximum sensitivity perpendicular to and parallel to the load direction, respectively. Only one PVDF NiCr sensor was located on coupon 02-06 with its direction of maximum sensitivity along the load direction, as shown in Figure 1. Note that the ultrasonic C-scanning was undertaken from the impact side of the coupons [6].

The "inverted", and therefore compression dominated, FALSTAFF fighter aircraft sequence [7] was applied to fatigue the coupon. Coupon 02-05 experienced a maximum compressive in-plane load level of -168 kN, which corresponds to a far-field strain of 3400 $\mu\epsilon$, for 106 programs. The load was decreased to -164 kN for the next 24 programs and then increased to -170 kN, i.e. 3430 $\mu\epsilon$, for a further 5 programs. To slow damage growth the load was once again lowered to -168 kN and remained at this level until failure occurred. Coupon 02-06 was subjected to a load of -170kN, which corresponded to a far-field strain of 3410 $\mu\epsilon$.

The tests were interrupted at intervals to produce ultrasonic C-scan maps and undertake piezoelectric measurements. C-scan maps gave an assessment of through-the-thickness damage in the composite. The peak-to-peak output voltage of the sensor was measured, under constant amplitude cyclic load levels of 0 ± 10 kN, 0 ± 20 kN and 0 ± 30 kN at 3 Hz, using a charge amplifier and a Nicolet digital storage oscilloscope.

3.1.2 Composite-to-Metal Fastened Joints

To simulate a mechanically fastened composite-to-metal joint, a composite coupon of dimensions 50 x 220 x 6.7 mm was tested together with a metal fixture, see Figure 2 [8]. The composite coupon was first drilled through using a 6.2 mm tungsten carbide double fluted drill, then reamed and counter sunk with 100° countersink and finally relieved at about the mid-ply layer with a 50° countersink. The two fastener holes, designated "A" and "B", were placed in line along the axis of the coupon as shown in Figure 2. The fasteners were installed in the coupon and fixture and tightened to a torque of 10 Nm. Full assembly details are given in Saunders et al [9]. Each coupon was inspected prior to and during the fatigue testing program using a time-of-flight ultrasonic C-scanning method [6].

The purpose of this test was to measure changes in the load path during the fatigue program. In order to achieve this, several piezoelectric sensors were positioned as shown in Figure 3. These sensors were made from NiCr sputtered PVDF film and applied using Versilok 201 acrylic adhesive. The sensors F2 and B2, on coupon 04-07, covered a substantial area between the two holes and thus measured surface area changes due to the by-pass loads and the compressive bearing loads. Sensors F1 and B1 measured bearing strains and hoop strains around hole A. The direction of maximum sensitivity of the PVDF film corresponds to the applied load direction.

The fixtures were subjected to sequence loading, where the load sequence used was the McDonnell Douglas (MCAIR) 300 hour program (MACSEQ). The peak loads applied to the coupons were derived from MCAIR wing fold strain (load) data and were then factored by 1.37. This corresponded to a tension-dominated loading sequence with a peak tensile/compressive in-plane load of 36/23 kN.

The tests were interrupted at intervals to produce ultrasonic C-scan maps and undertake piezoelectric measurements. Peak-to-peak piezoelectric voltage measurements were measured at two cyclic loading conditions, viz. tension-compression cyclic load of 0 ± 10 kN and tension-tension cyclic load of 10 ± 10 kN, at 3 Hz.

3.2 Results and Discussion

3.2.1 Impact Damaged Laminates

Figures 4 and 5 show the variation in damage area and normalised piezoelectric sensor output with increasing number of FALSTAFF programs for coupons 02-05 and 02-06, respectively. Note that the ratio of damage area, $(A_n - A_0)/A_0$, has been plotted, where A_0 and A_n are the damage areas measured at program 0 and n , respectively. Sensor PZF1, on coupon 02-05, was orientated such that it was sensitive to width-wise changes in area, hence the signal from PZF1 was a factor of 10 less than that measured from PZF2. Therefore any apparent changes in PZF1, as shown in Figure 4, always appeared to be within the region of noise of the sensor, thus no meaningful results can be attained from this sensor.

Sensor PZF2, which measured integrated changes in displacement along the load direction, showed steady sensor output voltages until program 90 where a 5% decrease in signal was detected, this coincided with an increase in measured damage area of 15 %, see Figure 4. The applied load was then reduced at program 106 to -164 kN in an effort to slow damage growth. This adjustment in load appeared to retard damage growth, as was observed by both the C-scans and PZF2 outputs. The load was then increased, at program 130, to -170 kN. Consequently, damage growth increased substantially, after only 5 programs, with a 10% increase in damage area and a 7% decrease in PZF2 output. So far, an overall increase in damage area of 27% has caused a reduction in PZF2 output of about 10%. However, subsequent damage growth (up to 56%) did not appear to cause significant changes in sensor output. Note that the damage, in these composite coupons, tends to grow in an elliptical manner, with the major axis in the width-wise direction. The sensor on coupon 02-06 showed a 10% reduction in output for a 60% increase in damage area, as illustrated in Figure 5.

All sensors were placed on the non-impact side, i.e., the side of maximum delamination damage since the impact damage takes a conical form with the base on the non-impact side. In a previous series of tests, Bennett et al [10] conducted an investigation using piezoelectric sensors on the impact side of the coupon which found an increase in sensor output from sensors over the damage area compared to those in the far-field. It was concluded that these sensors were measuring the compliance changes due to damage. One would expect that, even for the case here, the sensor output would increase with increasing size in damage. The decrease in piezoelectric sensor output that occurs here is probably due to complex non-linear surface effects. For example, under compressive in-plane loading "local buckling" occurs in the damage region, on the non-impact side, causing an out-of-plane surface

displacement. Thus the piezoelectric sensor would measure a combination of in-plane compressive deformation and tensile deformation possibly resulting in a lower sensor output.

The present results show definite trends in sensor output as damage grows within the coupon. As a result, this work reinforces the previous choice of attaching the piezoelectric sensors to the impact side of the coupon [10]. This has greater potential for monitoring the local structural compliance.

3.2.2 Composite-to-Metal Fastened Joints

Figure 6 shows typical piezoelectric signals for coupon 04-07, as well as the corresponding C-scans. These figures show time varying signals for the coupons as the number of simulated flight hours increase. Ultrasonic C-scanning is a useful method in determining the extent of damage and the through-the-thickness damage state. However this technique is limited because it can only detect damage which extends past the countersunk region since the countersink obscures any damage which may occur underneath it. The fasteners in coupon 04-07 failed during program 11, after which the test was terminated.

The interpretation of the signals in Figure 6 is complicated. For example, for sensor B2, when a tensile load was applied the main areas of deformation measured were a combination of compressive (bearing) near hole B and tensile in the region between the holes and toward the coupon edge due to loads by-passing hole B. When a compressive load was applied, sensor B2 was subjected to compressive loads by-passing hole B as well as compressive (bearing) loads around hole A. The changes in signals, observed in these figures, with increasing number of applied MACSEQ programs are the result of a number of factors, viz., changes in compliance due to damage, hole elongation causing fastener tilt, variations in fastener clamping forces and changes in load path.

Figure 7 shows variations in the normalised piezoelectric sensor voltages, V_n/V_0 taken at the load case 0 ± 10 kN, with increasing number of applied MACSEQ programs for coupon 04-07. Here V_n and V_0 are the peak-to-peak piezoelectric sensor voltages at program n and 0 respectively. The increase in sensor output for B2 and F2, i.e. sensors between holes A and B, is due to changes in by-pass loads and increases in compliance of the composite material between the holes (see Figure 7). Changes of up to 60 and 14% were measured for the two sensors, respectively, before fastener failure occurred. Optical microscopic studies of cross-sectioned composite coupons [9] have shown that the back side of the composite coupon is more likely to suffer damage, due to fastener rocking, hence this side should experience the greater change in signal, as was found in Figure 7 for sensor B2.

In summary, the results for coupon 04-07, shown in Figure 7, indicated that this technology has the potential to measure variations in the by-pass loads.

4. CRACKED METALLIC SPECIMEN

4.1 Experimental Setup

The specimen used, shown in Figure 8, was an aluminium alloy (US alloy 2214) centre-cracked-tension specimen subjected to constant amplitude, cyclic loading. The specimen was 12.5 mm thick. A mean load of 40 kN with a constant cyclic amplitude of 20 kN, at frequency of 5 Hz, was applied. The crack growth resulting from this cyclic loading was measured periodically with a travelling vernier microscope.

A number of NiCr sputtered 28 μm thick piezoelectric sensors, of dimension is 4 x 20 mm, were located on the specimen as shown in Figure 8. An epoxy adhesive was used to adhere the sensors to the aluminium specimen. The signal from sensor C (see Figure 8), which is located away from the "damage" area, is used as a reference signal and is known as the "far-field" signal. The "near-field" signals are obtained from sensors A and B. Since piezoelectric sensors are dynamic devices, the sensor readings were obtained under cyclic loading at a frequency of 5 Hz. The sensor output was conditioned using a charge amplifier and the peak-to-peak voltage readings were measured using a digital storage oscilloscope. After a predetermined number of loading cycles the crack length and peak-to-peak sensor voltages were measured. In this report, the crack length is the distance from the edge of the hole to the crack tip.

4.2 Numerical Analysis

To support the experimental results, the change in the piezoelectric sensor reading with crack growth was predicted numerically using Finite Element Analysis. Due to symmetry, only a quarter of the specimen was modelled using 15 and 20 noded isoparametric brick elements, as illustrated in Figure 9. The end loads and constraints used were similar to those applied in the experiment. The output from the piezoelectric sensor is related to the surface strains as shown below.

The output voltage from a piezoelectric sensor is expressed in equation (1). The surface strains on the aluminium are the same as those in the film since the bond is thin and rigid, thus the stresses in the piezoelectric film can be expressed in terms of the surface strains of the aluminium alloy, viz.:

$$V = (A_1 + A_2(1+K_2/K_1)) K_1 E_f \int \epsilon_{1f} dA + (A_2+K_2/K_1(A_1+A_2)) K_1 E_f \int \epsilon_{2f} dA \quad (2)$$

where $A_1=1/(1+\nu)$ and $A_2=\nu/((1+\nu)(1-\nu))$, ν is the Poisson ratio of the piezoelectric film, E_f is the modulus of elasticity of the film, and ϵ_{1f} and ϵ_{2f} are the strains in the sensor. It must be pointed out at this stage that the formulation in equation (2) only holds if the piezoelectric film is mechanically isotropic; an assumption which is made

for the purpose of this investigation. To model the electromechanical anisotropy, the ratio of (K_2/K_1) is assumed to be 0.125 [4], E_f is 2 GPa and a Poisson's ratio of 0.4 is assumed. Equation (2) should be sufficient to model the output from a piezoelectric sensor when it is located over an uncracked region. However, in the event of the crack propagating under the sensor the formulation in equation (2) should include the effects of the crack opening. Here the total signal obtained from the piezoelectric sensor should be a sum of two components, viz., (1) from the sensor over the crack opening, (i.e. behind the crack tip) and (2) from the remainder of the sensor. In this case, the total output voltage can be expressed as;

$$V = \left\{ (A_1 + (1 - \nu)A_2)K_1E_f \int \epsilon_{1f} dA \right\}_{\text{over-crack}} +$$

$$\left\{ (A_1 + A_2(1 + K_2/K_1)) K_1 E_f \int \epsilon_{1f} dA + \right.$$

$$\left. (A_2 + K_2/K_1(A_1 + A_2))K_1 E_f \int \epsilon_{2f} dA \right\}_{\text{(remainder)}} \quad (3)$$

In the results presented in this paper, the sensitivity of the piezoelectric sensor is defined as;

$$\text{sensitivity} = V_A/V_C \text{ or } V_B/V_C \quad (4)$$

where V_A , V_B and V_C are the signals obtained from piezoelectric sensors A, B and C, respectively, as shown in Figure 8.

It is evident from equation (3) that the output from the piezoelectric sensor can be expressed in terms of the surface strains measured on the specimen. Therefore the sensor output is a direct measure of the severity of the crack.

4.3 Results and Discussions

Figure 10 shows the crack growth measured in the specimen with increasing number of applied cycles. The variation of the piezoelectric sensor outputs with increasing crack length are shown in Figure 11. Note that the sensor signal undergoes a change in its gradient when the crack propagates under the sensor, as shown in curve (B) of Figure 11. This is due to the changes in stress states in the piezoelectric sensor as will be discussed below.

Figures 12(a) and (b) show the comparison between the predicted signal and the measured signal with increasing crack length. The agreement between the two results confirms the ability of a piezoelectric sensor to monitor the crack growth. The change in gradient observed in curve (B) of Figure 11 is attributed to the change in the stress state in the piezoelectric sensor when the crack propagates under the sensor.

Figure 13 shows the contribution of the two components described in equation (3) to the total piezoelectric sensor signal. This figure also reveals that when the crack propagates past the sensor the first term of equation (3) dominates. In this case, the rest of the sensor is located in a region of decreasing load. The piezoelectric sensor is therefore seen to be capable of detecting the change in the stress field due to the presence of a crack, even though the crack tip may be distant from the sensor. The slope of the sensitivity curve changes when the crack propagates past the sensor. The total sensor output in the latter case is an indication of the crack opening displacement.

5. CONCLUSIONS

Piezoelectric sensors show promise as an "active" technique for monitoring the condition of the composite-to-metal mechanically fastened joints tested in this investigation. These sensors were used to monitor variations in the by-pass loads in the joint, thus giving an assessment of the condition of the joint.

For the damage growth tests undertaken, the piezoelectric sensor output showed definite trends as damage grows within the composite. The present work supports the concept, presented in [10], of attaching the piezoelectric sensors to the impact side of the coupon and incorporating small sensors.

In a "real" aircraft structure it is evident that the piezoelectric film can be used as a sensor to detect structural damage. It is believed that the sensor detects changes in the compliance of the structure.

The ability of piezoelectric sensors to detect and monitor crack growth in metals was also shown. The results have also confirmed the constitutive relationship used to relate the stress/strain state in the structure to the piezoelectric sensor output.

ACKNOWLEDGEMENTS

The authors wish to acknowledge the assistance of Carlos Rey, Michael Ryan, Lewis Samutt and Gary Deirmendjian with the experimental program. Special thanks to Bruce Bishop and Howard Morton for their assistance with the C-scanning.

REFERENCES

1. Rogers, C.A., D.K. Barker and C.A. Jaeger, 1988. "Introduction to Smart Materials and Structures," *Proceedings of ARO Smart Materials, Structures and Mathematical Issues Workshop, VPI & SU, Blacksburg, VA, Sept. 1988.*, pp. 17-28.
2. Ahmad, I., 1988. "Smart Structures and Materials," *Proceedings of ARO Smart Materials, Structures and Mathematical Issues Workshop, VPI & SU, Blacksburg, VA, Sept. 1988.*, pp. 13-16.
3. Takagi, T., 1990. "A Concept of Intelligent Materials," *Proceedings of US-Japan Workshop on Smart/Intelligent Materials and Systems, University of Hawaii, Honolulu, 19-23 March, 1990.*
4. Atochem N.A., 1987. *Kynar Piezo Film Technical Manual*, Atochem N.A. - Piezo Film Sensor Division, Valley Forge, PA.
5. Lee, C.K. and O'Sullivan, T.C., 1990. "Piezoelectric strain gages," *IBM Research Rept*, RJ 7636 (71083).
6. Galea, S.C. and D.S. Saunders, 1992. "In-situ ultrasonic C-scanner," *ARL-TR-4*, DSTO Aeronautical Research Laboratory, Melbourne, Australia, November 1992.
7. Saunders, D.S., G. Clark, T.J. van Blaricum and T.E. Preuss, 1990. "Graphite/Epoxy Coupon Testing Program," *Theoretical and Applied Fracture Mechanics*, Vol. 13, pp. 105-124.
8. Saunders, D.S., M.G. Stimson, E. Kowal and C. Rey, 1990. "Preliminary Investigations of the Static Failure and Fatigue Behaviour of Mechanical Joints in Composite Materials," *ARL-STRUCT-TM 572*, DSTO Aeronautical Research Laboratory, Melbourne, Australia, October 1990.
9. Saunders, D.S., S.C. Galea and G.K. Deirmendjian, 1993. "The Development of Fatigue Damage around Fastener Holes in Thick Graphite/Epoxy Composite Laminates," *Composites*, Vol 24, No 4, pp. 309-321.
10. Bennett, J., J. Paul, R. Jones and A. Goldman, 1991. "A Preliminary Study on Damage Detection using Piezoelectric Film," *ARL-STRUCT-TM 538*, DSTO Aeronautical Research Laboratory, Melbourne, Australia, November 1991.

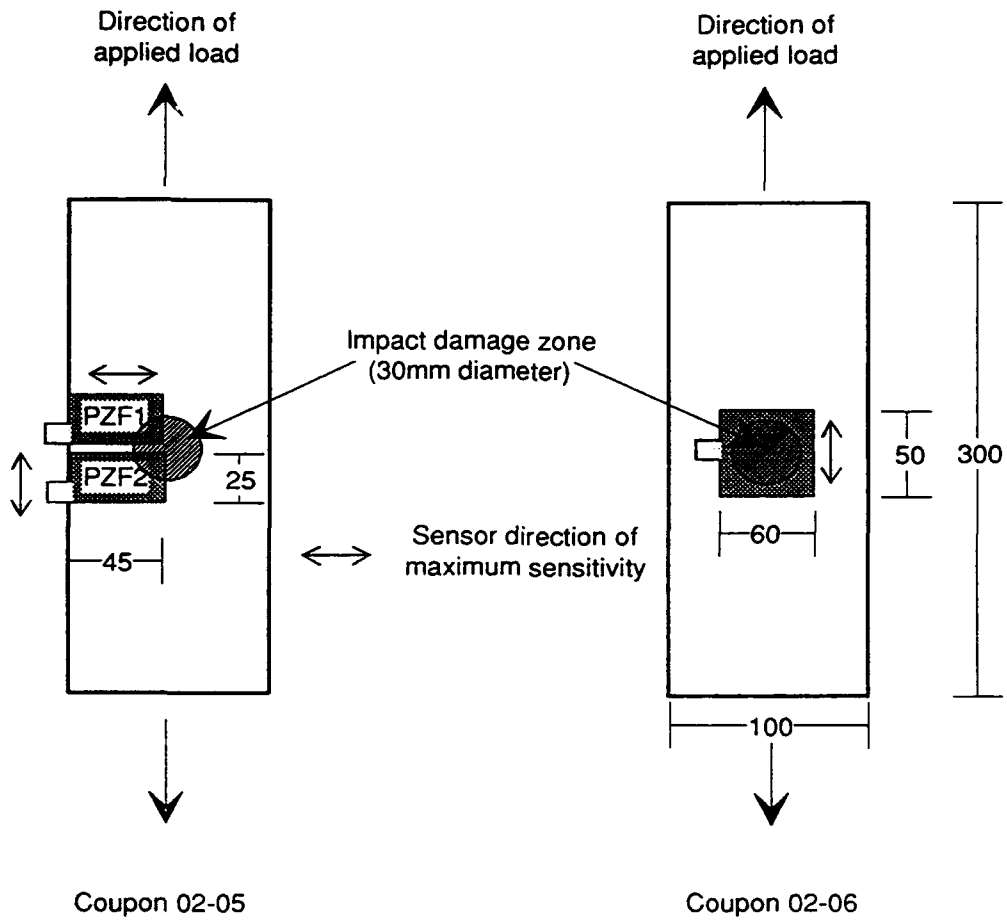


Figure 1: Location and size of the piezoelectric sensors on the non-impact side of an impact damaged composite coupon (all dimensions in mm).

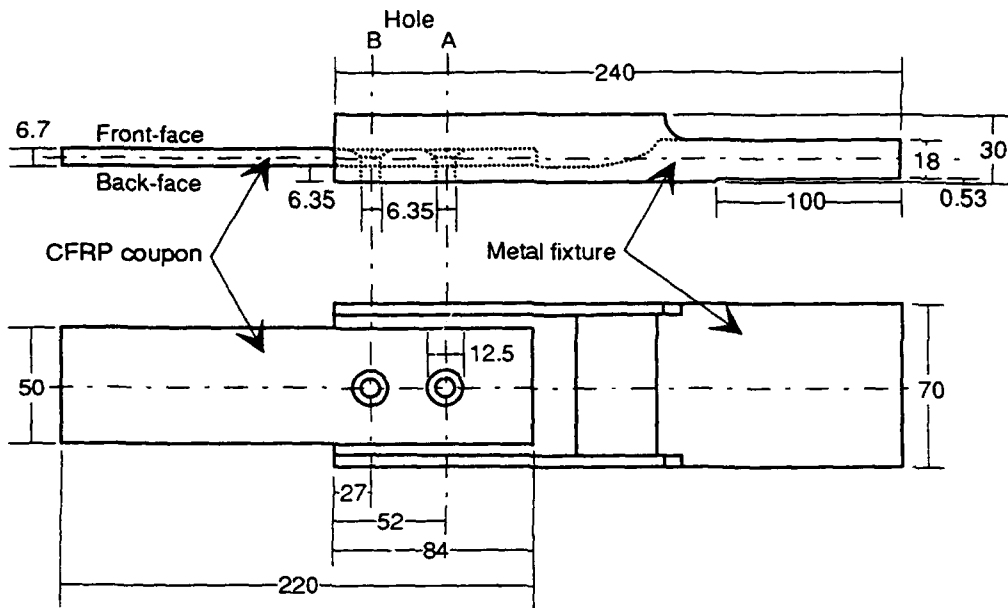


Figure 2: The composite-to-metal specimen configuration for the fatigue testing of mechanical fastened joints (all dimensions in mm).

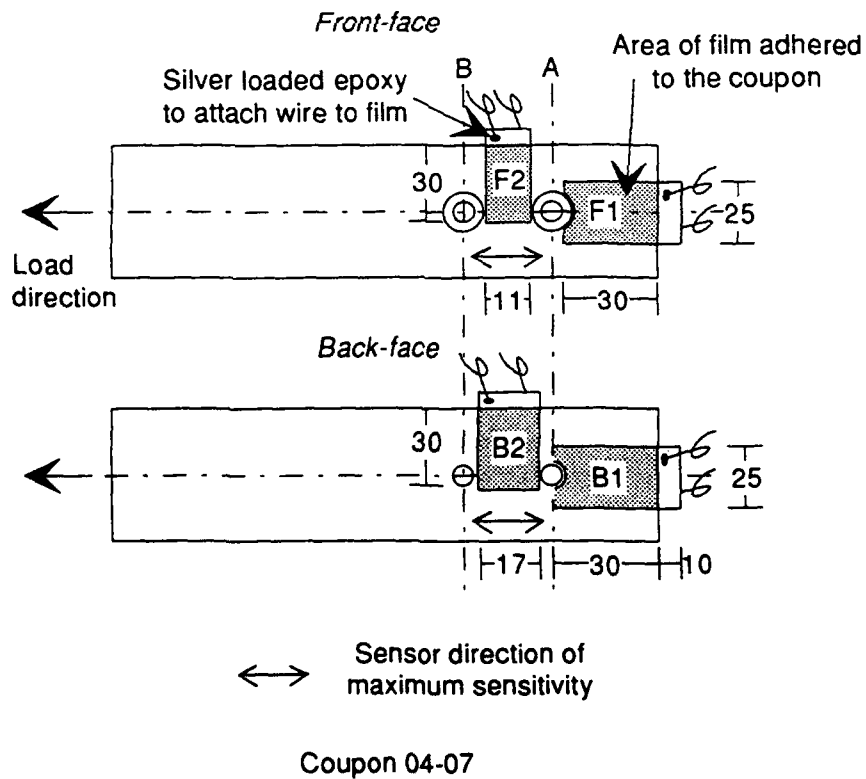


Figure 3: Location and size of piezoelectric sensors on the composite bolted joint coupons (all dimensions in mm).

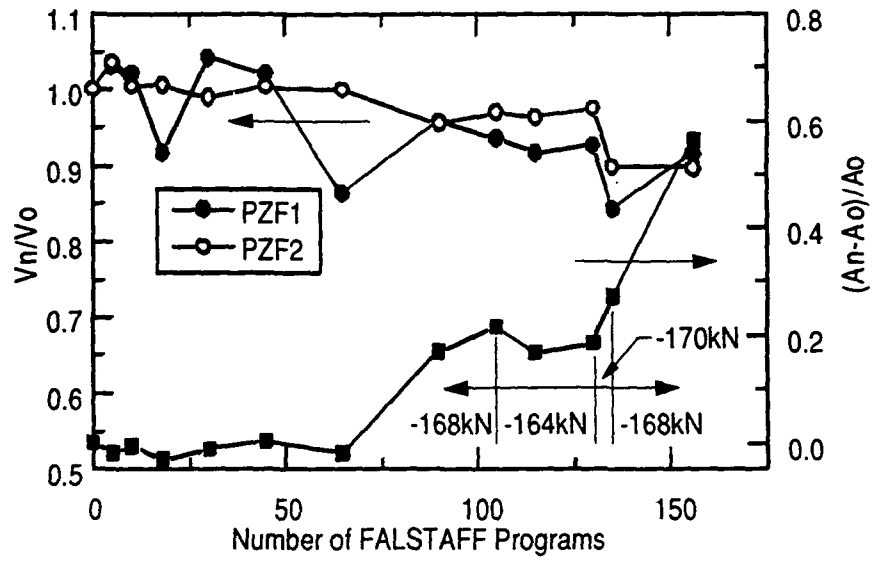


Figure 4: Variation of damage area and piezoelectric sensor outputs (for the load case 0 ± 10 kN) against number of FALSTAFF programs for coupon 02-05.

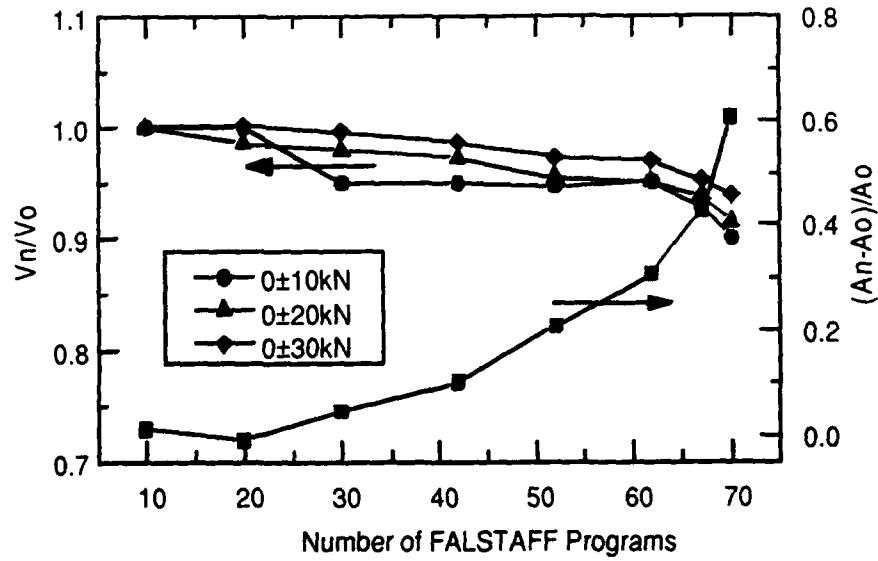


Figure 5: Variation of damage area and piezoelectric sensor outputs against number of FALSTAFF programs for coupon 02-06.

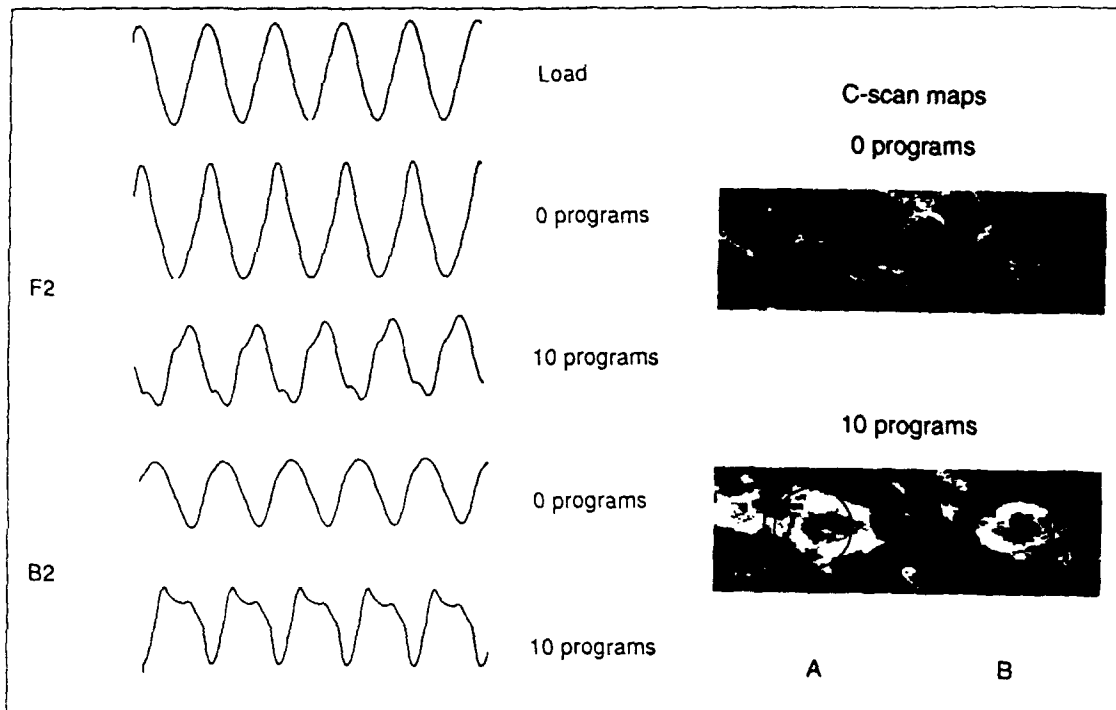


Figure 6: Typical signals from sensors F2 and B2 (0 ± 10 kN) on coupon 04-07 with the corresponding C-scans.

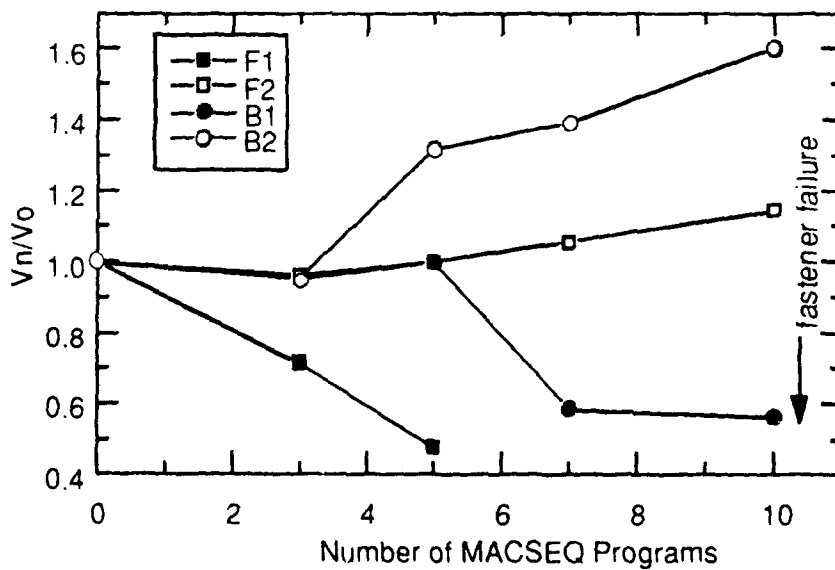


Figure 7: Variation of piezoelectric sensor outputs (for the load case 0 ± 10 kN) against number of MACSEQ programs for coupon 04-07.

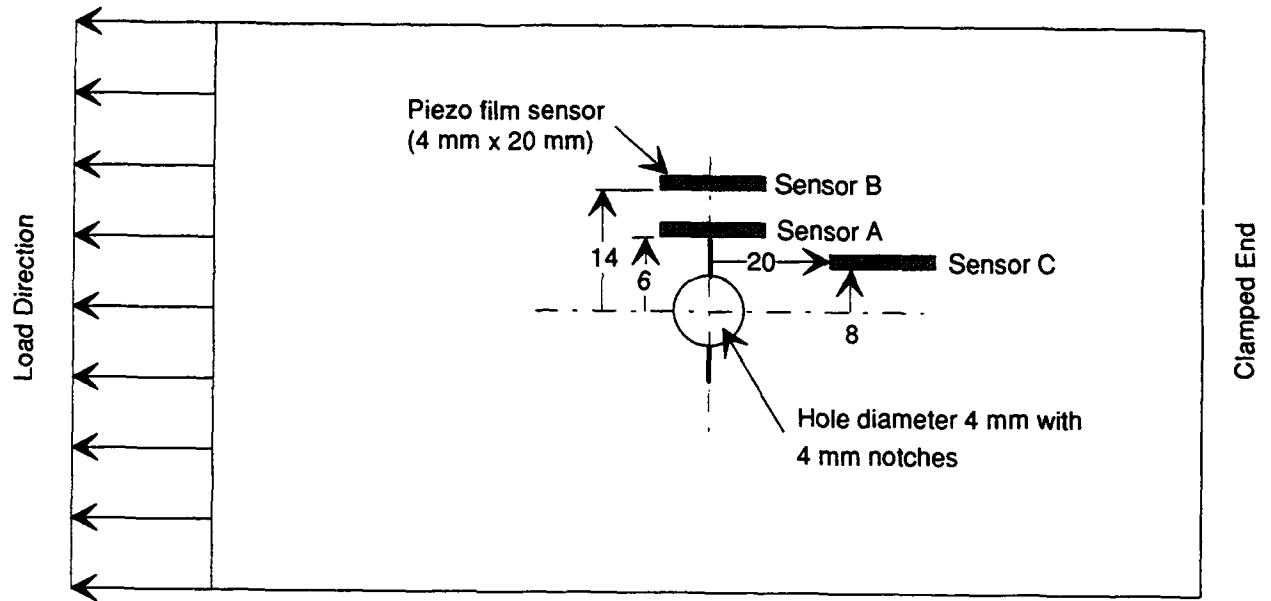


Figure 8: Schematic of the aluminium specimen (dimensions in mm)

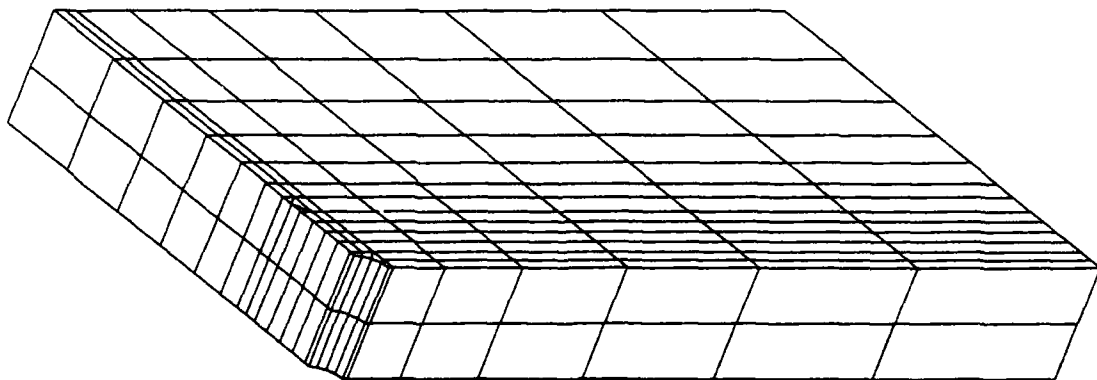


Figure 9: Finite element mesh for the aluminium specimen

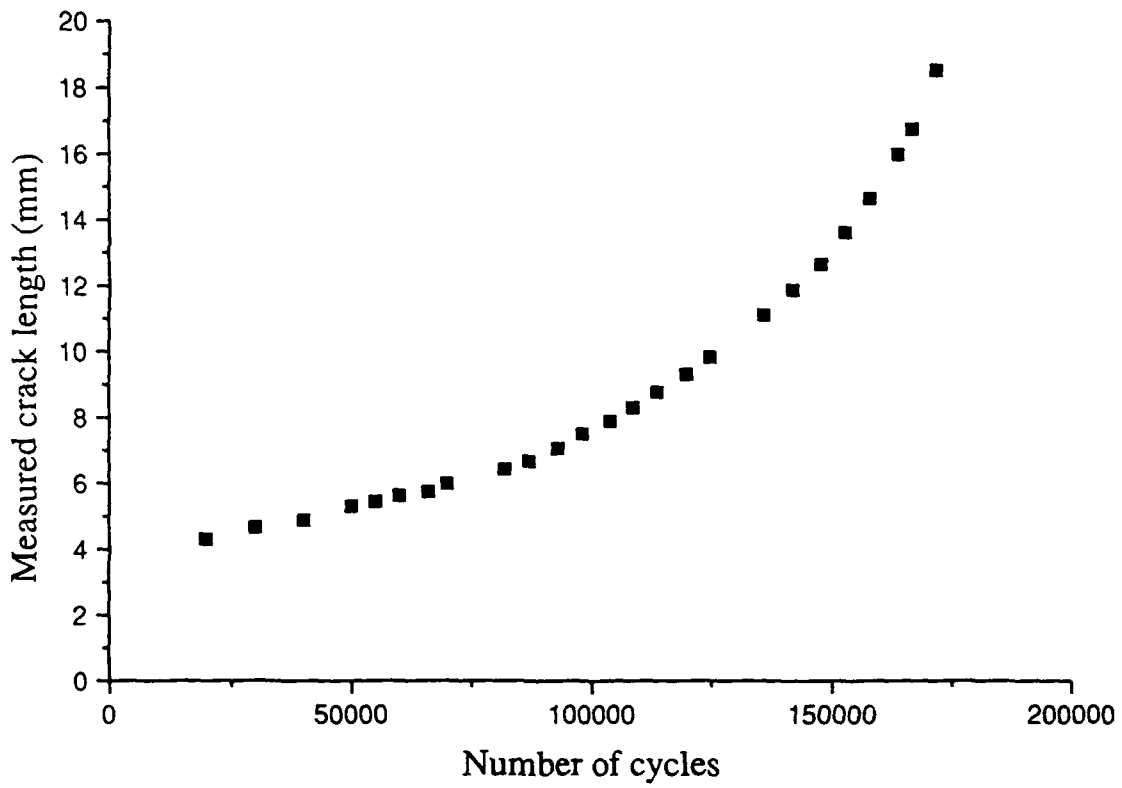


Figure 10: Measured crack growth versus number of applied cycles

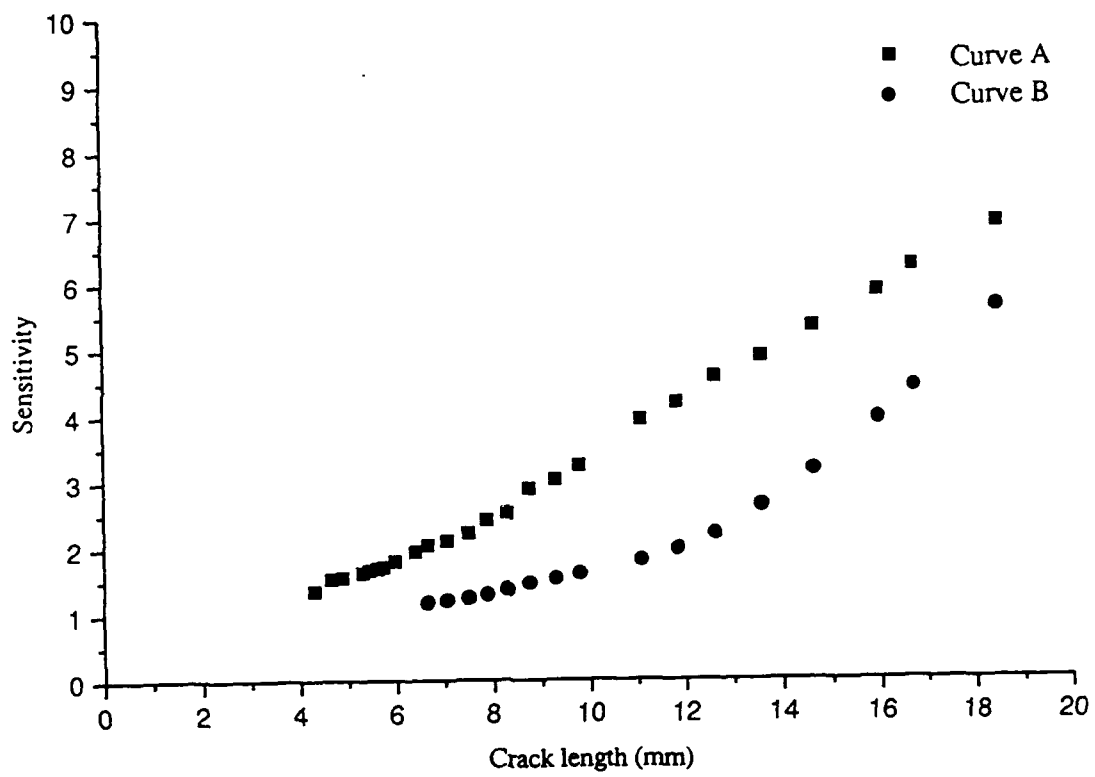
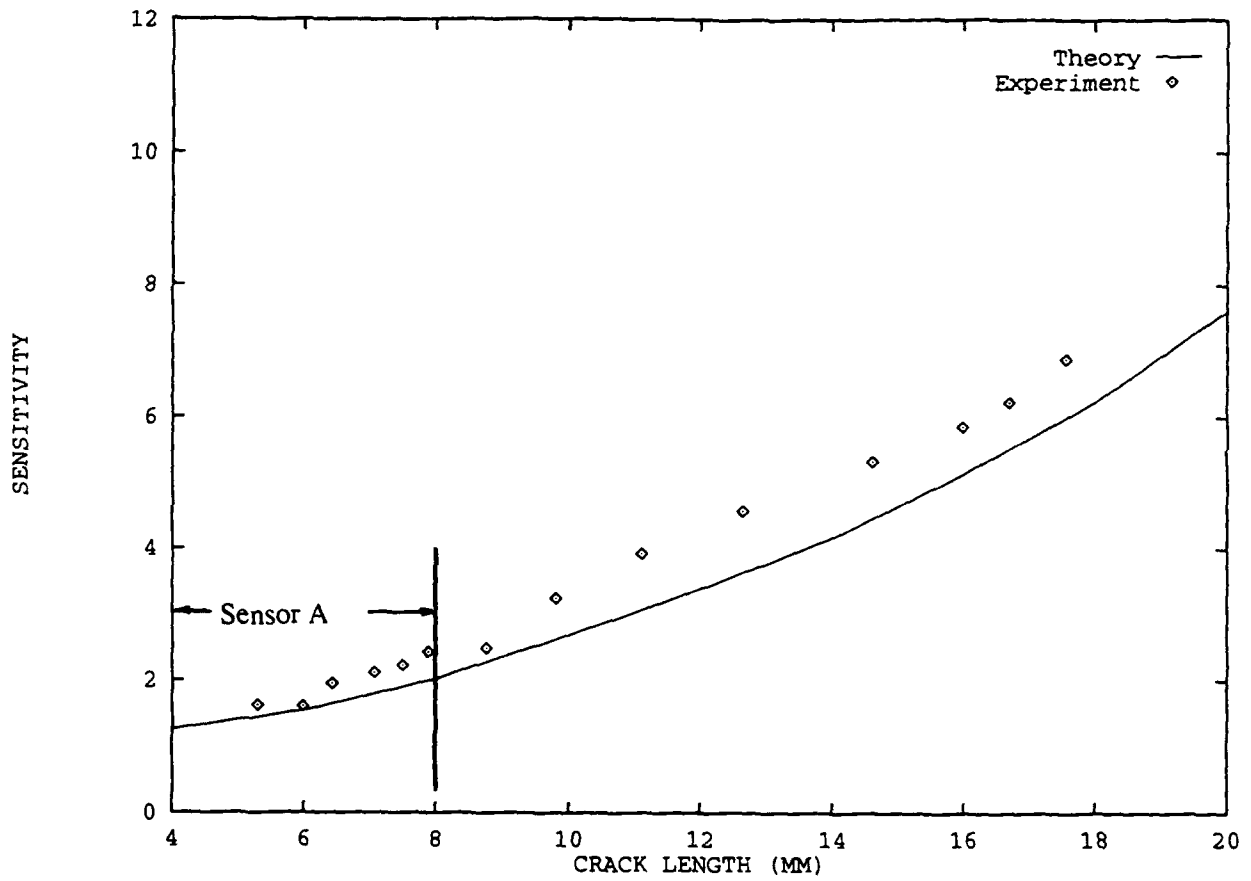


Figure 11: Piezo electric sensor output versus measured crack length.
 Curve A - V_A/V_C ; Curve B - V_B/V_C



(a)

Figure 12: Comparison between the predicted sensor output and the measured signals with increasing crack length. (a) V_A/V_C ; (b) V_B/V_C

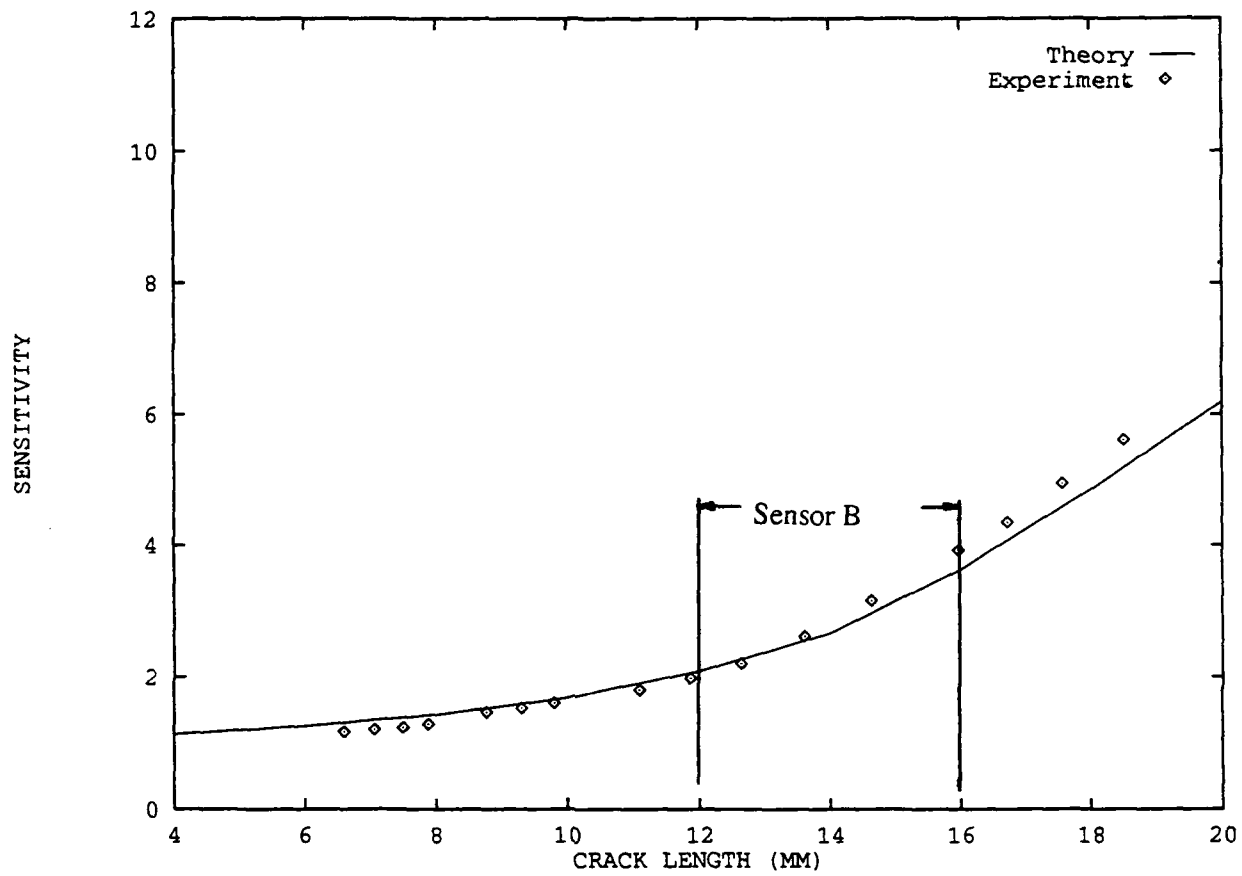
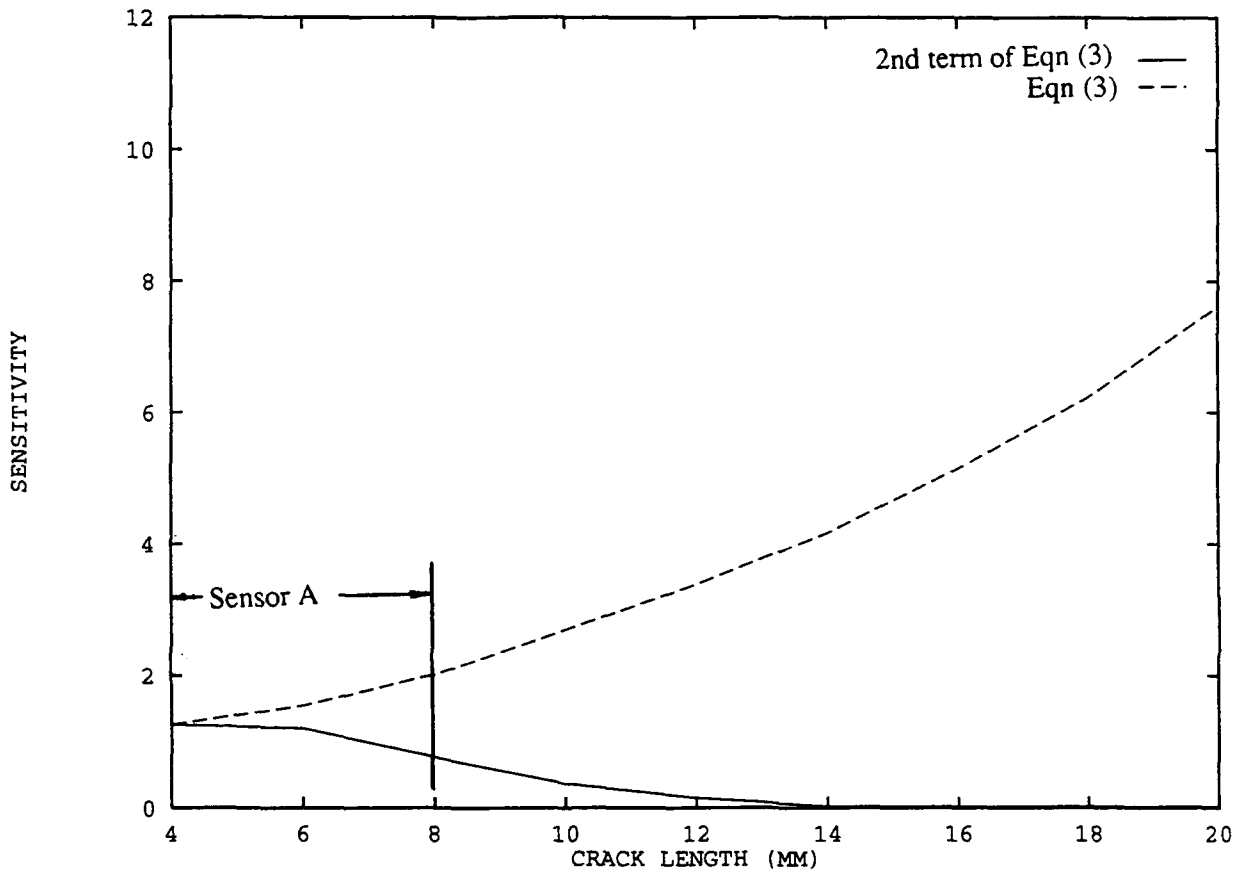


Figure 12 (b)



(a)

Figure 13: Contribution from the various components in Equation (3).
 (a) V_A/V_C (b) V_B/V_C

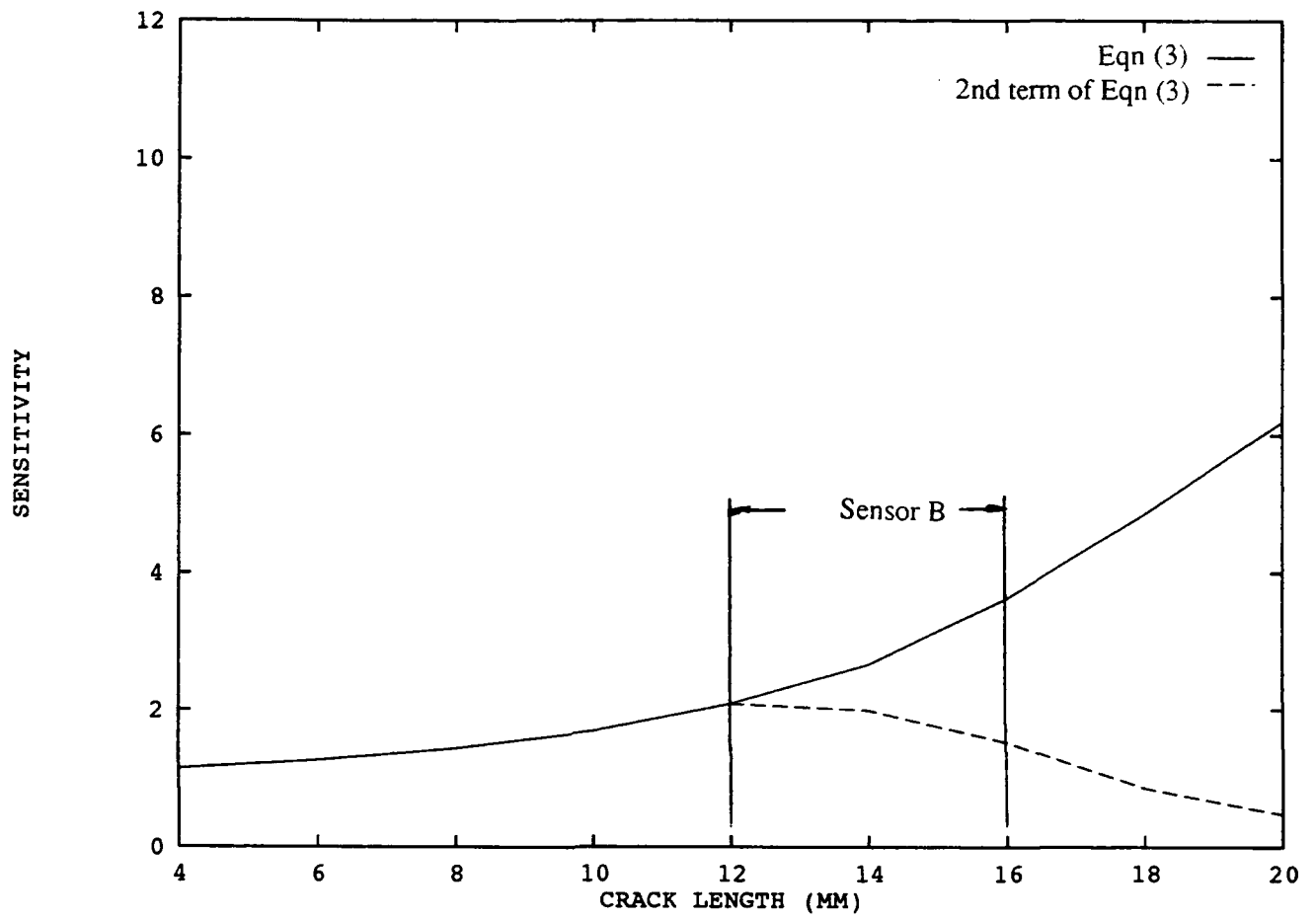


Figure 13 (b)

DISTRIBUTION

AUSTRALIA

Department of Defence

Defence Central

Chief Defence Scientist
AS, Science Corporate Management } shared copy
FAS Science Policy }
Counsellor, Defence Science, London (Doc Data sheet only)
Counsellor, Defence Science, Washington (Doc Data sheet only)
Scientific Adviser, Defence Central
OIC TRS, Defence Central Library
Document Exchange Centre, DSTIC (8 copies)
Defence Intelligence Organisation
Librarian, Defence Signals Directorate, (Doc Data sheet only)

Other Institutions

NASA (Canberra)
AGPS

Aeronautical Research Laboratory

Director
Library
Chief Airframes and Engines Division
Author: W.K. Chiu
S.C. Galea
M. Heller

Navy Office

Navy Scientific Adviser (3 copies Doc Data sheet only)

Army Office

Scientific Adviser - Army (Doc Data sheet only)

Air Force Office

Air Force Scientific Adviser
ARDU
Library
DENGPP-AF
DGELS OIC AME
OIC ATF, ATS, RAAFSTT, WAGGA (2 copies)

SPARES (3 COPIES)

TOTAL (29 COPIES)

PAGE CLASSIFICATION
UNCLASSIFIED

PRIVACY MARKING

DOCUMENT CONTROL DATA

1a. AR NUMBER AR-008-342	1b. ESTABLISHMENT NUMBER ARL-RR-4	2. DOCUMENT DATE MAY 1993	3. TASK NUMBER AIR 91/056						
4. TITLE DAMAGE MONITORING IN METALLIC AND COMPOSITE STRUCTURES USING PIEZOELECTRIC THIN FILM SENSORS		5. SECURITY CLASSIFICATION (PLACE APPROPRIATE CLASSIFICATION IN BOX(S) IE. SECRET (S), CONF. (C), RESTRICTED (R), LIMITED (L), UNCLASSIFIED (U)). <table border="1"> <tr> <td>U</td> <td>U</td> <td>U</td> </tr> <tr> <td>DOCUMENT</td> <td>TITLE</td> <td>ABSTRACT</td> </tr> </table>	U	U	U	DOCUMENT	TITLE	ABSTRACT	6. NO. PAGES 22 7. NO. REFS. 10
U	U	U							
DOCUMENT	TITLE	ABSTRACT							
8. AUTHOR(S) W.K. CHIU S.C. GALEA		9. DOWNGRADING/DELIMITING INSTRUCTIONS Not applicable.							
10. CORPORATE AUTHOR AND ADDRESS AERONAUTICAL RESEARCH LABORATORY AIRFRAMES AND ENGINES DIVISION 506 LORIMER STREET FISHERMENS BEND VIC 3207		11. OFFICE/POSITION RESPONSIBLE FOR: RAAF DENGPOL-AF SPONSOR _____ SECURITY _____ DOWNGRADING _____ APPROVAL _____ CAED							
12. SECONDARY DISTRIBUTION (OF THIS DOCUMENT) Approved for public release. OVERSEAS ENQUIRIES OUTSIDE STATED LIMITATIONS SHOULD BE REFERRED THROUGH DSTIC, ADMINISTRATIVE SERVICES BRANCH, DEPARTMENT OF DEFENCE, ANZAC PARK WEST OFFICES, ACT 2601.									
13a. THIS DOCUMENT MAY BE ANNOUNCED IN CATALOGUES AND AWARENESS SERVICES AVAILABLE TO . . . No limitations.									
13b. CITATION FOR OTHER PURPOSES (IE. CASUAL ANNOUNCEMENT) MAY BE <input checked="" type="checkbox"/> UNRESTRICTED OR <input type="checkbox"/> AS FOR 13a.									
14. DESCRIPTORS OH-58C helicopters Aviation accidents Australian Army Aviation Centre			15. DISCAT SUBJECT CATEGORIES 010301 0102						
16. ABSTRACT <i>The increasing emphasis on intelligent material systems and structures has resulted in a significant research effort in the areas of embedded and bonded sensors and actuators. Piezoelectric film are one of the many sensing materials available. The piezoelectric sensor output is proportional to changes in surface displacement and can be used to interpret variations in structural and material properties, e.g., the compliance of the structure. The aim of this paper is to demonstrate the use of piezoelectric film sensors as a structural integrity monitoring device for detecting damage in fibre reinforced composites, and crack growth in aluminium alloy specimens.</i>									

PAGE CLASSIFICATION
UNCLASSIFIED

PRIVACY MARKING

THIS PAGE IS TO BE USED TO RECORD INFORMATION WHICH IS REQUIRED BY THE ESTABLISHMENT FOR ITS OWN USE BUT WHICH WILL NOT BE ADDED TO THE DISTIS DATA UNLESS SPECIFICALLY REQUESTED.

16. ABSTRACT (CONT.)

17. IMPRINT

AERONAUTICAL RESEARCH LABORATORY, MELBOURNE

18. DOCUMENT SERIES AND NUMBER

Research Report 4

19. WA NUMBER

21 218F

20. TYPE OF REPORT AND PERIOD COVERED

21. COMPUTER PROGRAMS USED

22. ESTABLISHMENT FILE REF(S)

23. ADDITIONAL INFORMATION (AS REQUIRED)